

The Spectroscopic, Electrochemical and Structural Characterization of a Family of Ru Complexes Containing the C_2 -Symmetric Didentate Chiral 1,3-Oxazoline Ligand and Their Catalytic Activity

Xavier Sala,^[a] Naiara Santana,^[a] Isabel Serrano,^[a] Elena Plantalech,^[a] Isabel Romero,^[a] Montserrat Rodríguez,^{*[a]} Antoni Llobet,^{*[b,c]} Susanna Jansat,^[d] Montserrat Gómez,^[d] and Xavier Fontrodona^[e]

Keywords: Ruthenium / N ligands / Epoxidation / Chiral ligands / Atropisomerism

The structural, spectroscopic, and electrochemical characterization and a preliminary catalytic investigation of a family of Ru^{II} complexes with general formula [Ru(Y)(terpy)(phbox-R)]ⁿ⁺ [where terpy is 2,2':6',2''-terpyridine, phbox-R is a C_2 -symmetric bidentate oxazoline ligand (R = Et or *i*Pr), and Y is a monodentate ligand], are discussed. The X-ray structure of [RuCl(terpy)(phbox-*i*Pr)]²⁺ has been solved and confirms, as we described recently, the predicted generation of the less

hindered atropisomer, which is determined by the conformation of the stereogenic centers in the bidentate ligand. The catalytic properties of the aquo complexes have been tested in epoxidation reactions, and moderate selectivity for the epoxides is obtained for styrene and *trans*-stilbene when using PhI(OAc)₂ as co-oxidant.

(© Wiley-VCH Verlag GmbH & Co. KGaA, 69451 Weinheim, Germany, 2007)

Introduction

C_2 -Symmetric bis(1,3-oxazolines) have received an increasing amount of attention over the last few years, as can be seen from the increasing number of publications dealing with this type of ligand.^[1] Since the first reports of the use of chiral oxazoline ligands in asymmetric catalysis,^[2] a great variety of oxazoline-based compounds have been synthesized and successfully tested as catalysts,^[3] and their coordination chemistry studied,^[4] mainly because of their ease of preparation and versatility.

Atropisomerism, where chirality is generated due to rotational restriction between two isomers containing axially chiral biaryl compounds,^[5,6] is a good way of obtaining efficient tools in asymmetric synthesis^[6a,7] (for example the rigid molecular frameworks obtained from chiral ligands like BINAP^[8]), and has found important applications in diverse areas such as liquid crystals, pharmaceuticals, nano-scale information storage, or biomimetic catalysis.^[9]

Transition metal complexes bearing oxazoline ligands have shown good activities and enantioselectivities in a myriad of catalytic organic syntheses involving metals such as Cu or Fe.^[10] However, the performance of oxazoline-containing ruthenium complexes as catalysts has been developed only very recently, and the number of contributions in this area is still limited.^[11] Their performance as asymmetric epoxidation catalysts with clean oxidants such as H₂O₂, where they show good results in terms of both chemo- and enantioselectivity, has been widely studied by Beller and co-workers.^[12]

Interest in polypyridylruthenium complexes stems from their multiple applications in scientific fields such as photophysics and photochemistry,^[13] catalysis,^[14] and bioinorganic chemistry.^[15] One of the main goals for this type of complex is the design of structures that allow the fine-tuning of their redox, absorption, and emission properties. Among redox properties, and especially from a catalytic perspective, one of the major aims is the design of Ru=O functional groups and analogues capable of reversibly accepting multiple electrons and protons within a relatively narrow potential range.^[16]

With all this in mind, we present here the complete characterization and catalytic activity of a family of ruthenium complexes bearing C_2 -symmetric oxazoline ligands, including two aquo complexes that are potential pre-catalysts for redox processes involving the above mentioned Ru=O group. The chirality of the complexes prepared is determined by the stereogenic centers in the oxazoline entities

[a] Departament de Química, Universitat de Girona, Campus de Montilivi, 17071 Girona, Spain

[b] Institut Català d'Investigació Química (ICIQ), Av. Paisos Catalans 16, 43007 Tarragona, Spain

[c] Departament de Química, Universitat Autònoma de Barcelona, Cerdanyola del Vallès, 08193 Barcelona, Spain

[d] Departament de Química Inorgànica, Universitat de Barcelona, Martí i Franquès 1–11, 08028 Barcelona, Spain

[e] Serveis Tècnics de Recerca, Universitat de Girona, Edifici P II, Campus Montilivi, 17071 Girona, Spain

Supporting information for this article is available on the WWW under <http://www.eurjic.org> or from the author.

but also by the chiral axes generated upon coordination of the ligand, which leads to atropisomeric forms.

Results and Discussion

Synthesis and Solid-State Structure

The complexes described here have the general formula $[\text{Ru}(\text{Y})(\text{terpy})(\text{phbox-R})]^{n+}$, where phbox-R is one of the two oxazoline ligands depicted in Figure 1 and Y is a monodentate ligand $[\text{Cl}, \text{H}_2\text{O}, \text{MeCN}, \text{pyridine (py)}, \text{or } 2\text{-hydroxypyridine (2-OH-py)}]$. The chlorido complexes $(R_cR_c, S_aR_a)\text{-2a}$ and $(S_cS_c, R_aS_a)\text{-2b}$ were obtained by reduction of $[\text{RuCl}_3(\text{terpy})]$ (**1**) in the presence of the appropriate bidentate oxazoline ligand, and the remaining compounds were derived from these two complexes or their aquo analogs $(R_cR_c, S_aR_a)\text{-3a}$ and $(S_cS_c, R_aS_a)\text{-3b}$. The nomenclature of the complexes, as explained in the Experimental Section, involves a variety of chiral configurations arising from (1) the stereogenic centers inherent to each oxazoline ligand (either *R,R* or *S,S*; see Figure 1), which are represented by the first two letters having a “c” subscript, and (2) the chiral axes generated upon coordination of the ligand to the ruthenium metal center, as symbolized by the two remaining letters of the nomenclature used, with an “a” subscript. The two latter letters correspond to the chiral axis involving the oxazolinyl ring *trans* to the terpy ligand and that involving the ring *trans* to the monodentate ligand Y, respectively. The formation of one or other isomer is determined by the configuration of the oxazoline ligand (see below).

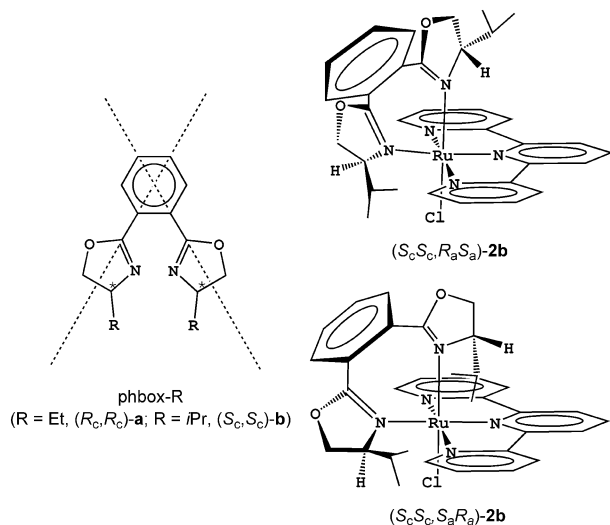


Figure 1. Atropisomers generated upon phbox-R ligand coordination.

The X-ray crystal structure for the cationic moiety of complex $(S_cS_c, R_aS_a)\text{-2b}$ is shown in Figure 2; Table 1 lists selected bond lengths and angles. Further crystallographic information for this structure can be found in the Experimental Section. This cation presents a highly distorted octahedral environment around the Ru metal center, with the

terpy ligand coordinating in a meridional fashion through its N atoms. Two of the remaining coordination sites are occupied by the didentate oxazoline ligand, whereas the sixth coordinative position is occupied by a chlorido ligand. The high distortion revealed in this cation is partly explained by the structural restrictions imposed by the terpy ligand coordination, which narrows the N1–Ru–N3 bond angle to 157.3° , far from the ideal value of 180° for a regular octahedral geometry.

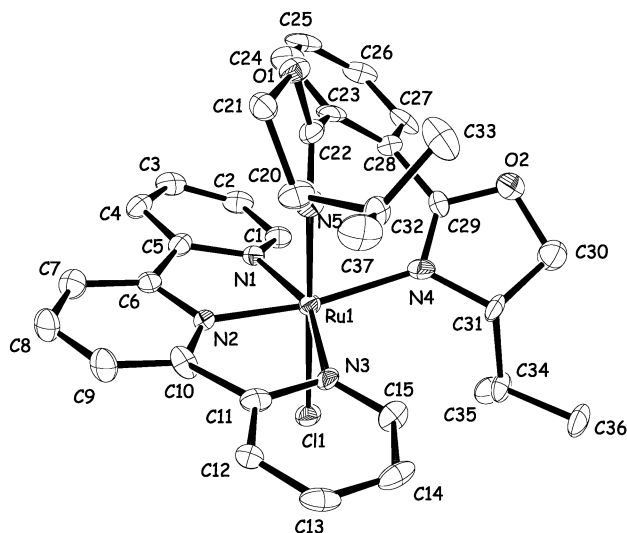


Figure 2. ORTEP plot (ellipsoids at 50% probability) of the cationic moiety of complex $(S_cS_c, R_aS_a)\text{-2b}$, including the atom numbering scheme.

Table 1. Selected bond lengths and angles for complex $(S_cS_c, R_aS_a)\text{-2b}$.

Bond lengths [Å]		Bond angles [°]	
Ru1–N1	2.042	N1–Ru1–N2	79.26
Ru1–N2	1.935	N1–Ru1–N3	157.34
Ru1–N3	2.126	N1–Ru1–N4	98.95
Ru1–N4	2.162	N1–Ru1–N5	90.97
Ru1–N5	2.035	N2–Ru1–N3	78.87
Ru1–Cl1	2.416	N2–Ru1–N4	170.06
		N2–Ru1–N5	87.31
		N3–Ru1–N4	103.62
		N3–Ru1–N5	93.86
		N4–Ru1–N5	82.93
		Cl1–Ru1–N1	87.28
		Cl1–Ru1–N2	92.71
		Cl1–Ru1–N3	87.90
		Cl1–Ru1–N4	96.98
		Cl1–Ru1–N5	178.21

Coordination of the phbox-*iPr* ligand, as described previously for analogous complexes,^[17] generates a seven-membered ring which is unlikely to keep a planar conformation because of structural restrictions. The ligand is thus forced to bend in order to accommodate itself upon coordination, and this bending leads to two possible atropisomeric configurations depending on the final orientation of the central phenyl ring of the phbox-*iPr* ligand, in other words over the N1 or N3 pyridyl rings of the terpy ligand (see Figure 1 for schematic drawings of the two possible conformations).

The coordination of the ligand also fixes its two oxazolanyl rings in a twisted position with regard to the central phenyl ring plane, thereby generating the two chiral axes depicted in Figure 1. The formation of one or the other atropisomer is governed by the configuration of the stereogenic centers (C20 and C31) of the oxazolanyl rings in such a way that only one atropisomer (the one that keeps the *i*Pr groups farthest away from the terpy plane) is found. The X-ray structural analysis of complex (S_cS_c,R_aS_a)-**2b** shows that the atropisomer generated is indeed the S_cS_c,R_aS_a one, as expected for an *S,S* configuration of the oxazoline ligand. The N4 and N5 oxazolanyl rings of the phbox-*i*Pr ligand are rotated by 51.47° and 40.26°, respectively, with regard to the central phenyl ring, and the N5–Ru–N4 angle is 82.93°.

The terpy ligand is not perfectly planar and experiments a slight twofold bending, with the two peripheral N1 and N3 pyridyl rings pointing away from the plane of the central N2 ring (the torsion angles are 8.64° and 7.7°, respectively, which gives an overall bending of 15.53° for the ligand). The rotation of the N1 ring of the terpy ligand with regard to the central pyridyl ring in terpy places it in an almost parallel disposition with regard to the central phenyl ring of the phbox-*i*Pr ligand (the angle between these two rings is 19.91°).

Finally, the cationic moieties in the crystal interact with one another through a series of hydrogen bonds that involve the chlorido ligand of one molecule and H7 and H13 of two neighboring molecules, with contact distances of 2.65 and 2.85 Å, respectively. These interactions arrange the complex molecules such that they form pseudo-square channels in the direction of the crystallographic *b* axis, which also allow a certain degree of π -stacking between the terpy ligands of adjacent entities (see the Supporting Information for diagrams of these 3D interactions).

Spectroscopic Properties

The UV/Vis spectra of complexes **2a,b**–**5a,b** and **6b** were recorded in dichloromethane and/or phosphate buffer solution. The main absorption wavelengths, together with their assignments, are listed in Table 2. The assignment of the spectral absorptions of Ru^{II} octahedral complexes has already been well documented^[18] and, accordingly, the set of highly energetic bands at wavelengths below 350 nm can be assigned to $\pi \rightarrow \pi^*$ intraligand transitions. Several charge-transfer $d\pi(\text{Ru}) \rightarrow \pi^*$ MLCT absorptions in the visible region of the spectra are also present for this family of compounds. These probably involve the π antibonding orbitals of terpy as the higher aromatic character of this ligand lowers its orbitals' energies with regard to the phbox-R ligand.

No significant differences can be found in Table 2 between analogous complexes containing the phbox-Et or the phbox-*i*Pr oxazoline ligands. However, the electronic nature of the monodentate Y ligand influences the energies of the transitions involving orbitals with $d_{(\text{Ru})}$ character to some extent. Thus, as expected, the π -donor character of the chlorido ligand increases the energy of the $d_{(\text{Ru})}$ filled orbitals, with complexes (R_cR_c,S_aR_a)-**2a** and (S_cS_c,R_aS_a)-**2b** being the ones that show the most red-shifted MLCT bands. Complexes **5** and **6**, which contain py and 2-OH-py ligands, respectively, show absorption energies similar to those found for the corresponding aquo complexes **3a,b**, therefore it can be concluded that the electron-withdrawing π effects of the corresponding aromatic systems in the pyridine-type ligands are minimal. This is consistent with the rapid ligand rotation determined in solution from NMR experiments.^[17]

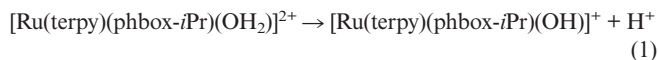
Finally, a comparison of these complexes with structurally similar Ru complexes also containing terpy reveals that, for complexes with bidentate oxazoline ligands,^[19] MLCT

Table 2. UV/Vis spectroscopic data for complexes **2a,b**–**5a,b** and **6b**.

Compound	Solvent	λ_{max} , nm (ϵ , M ⁻¹ cm ⁻¹)	Assignment
(R_cR_c,S_aR_a)- 2a	CH ₂ Cl ₂	282 (20360), 324 (26359) 370 (5617), 524 (5534), 570 (5202)	$\pi \rightarrow \pi^*$ $d\pi \rightarrow \pi^*$
(S_cS_c,R_aS_a)- 2b	CH ₂ Cl ₂	284 (23139), 322 (29822) 368 (6468), 530 (5342), 562 (5585)	$\pi \rightarrow \pi^*$ $d\pi \rightarrow \pi^*$
(R_cR_c,S_aR_a)- 3a	CH ₂ Cl ₂	282 (20215), 318 (28681) 475 (sh), 518 (4935)	$\pi \rightarrow \pi^*$ $d\pi \rightarrow \pi^*$
	phosphate buffer pH 7	280 (21538), 316 (25538) 470 (sh), 518 (4745)	$\pi \rightarrow \pi^*$ $d\pi \rightarrow \pi^*$
(S_cS_c,R_aS_a)- 3b	CH ₂ Cl ₂	278 (28320), 318 (29792) 486 (4989), 520 (4950)	$\pi \rightarrow \pi^*$ $d\pi \rightarrow \pi^*$
	phosphate buffer pH 7	264 (17983), 316 (23760) 467 (3296), 525 (3948)	$\pi \rightarrow \pi^*$ $d\pi \rightarrow \pi^*$
(S_cS_c,R_aS_a)- 4b	CH ₂ Cl ₂	280 (19150), 315 (18540), 327 (17340) 383 (5970), 412 (5980), 541 (4730), 567 (sh)	$\pi \rightarrow \pi^*$ $d\pi \rightarrow \pi^*$
(R_cR_c,S_aR_a)- 5a	CH ₂ Cl ₂	276 (22429), 318 (30269) 370 (sh), 475 (sh), 518 (5162)	$\pi \rightarrow \pi^*$ $d\pi \rightarrow \pi^*$
(S_cS_c,R_aS_a)- 5b	CH ₂ Cl ₂	278 (26080), 318 (35425) 370 (sh), 470 (sh), 512 (5690)	$\pi \rightarrow \pi^*$ $d\pi \rightarrow \pi^*$
(S_cS_c,R_aS_a)- 6b	CH ₂ Cl ₂	276 (26120), 316 (30050) 377 (sh), 494 (3920), 534 (sh)	$\pi \rightarrow \pi^*$ $d\pi \rightarrow \pi^*$

transitions generally take place at much lower energies than those of analogous complexes having aromatic bidentate ligands,^[20] thereby manifesting the increased electron-donor capacity of the oxazoline entities.

Acid-base titration was performed on complex (S_cS_c, R_aS_a)-**3b** by slow addition of NaOH to an acidic aqueous solution of the complex [Equation (1)].



The initial and final UV/Vis spectra, together with several intermediate spectra (inset), are displayed in Figure 3. The MLCT bands shift to longer wavelengths (520 and 518 nm) upon deprotonation of the aquo ligand, in agreement with the relative destabilization of the $d\pi(\text{Ru})$ levels provoked by the anionic hydroxido ligand in a similar way to that described above for the chlorido ligand.^[20d]

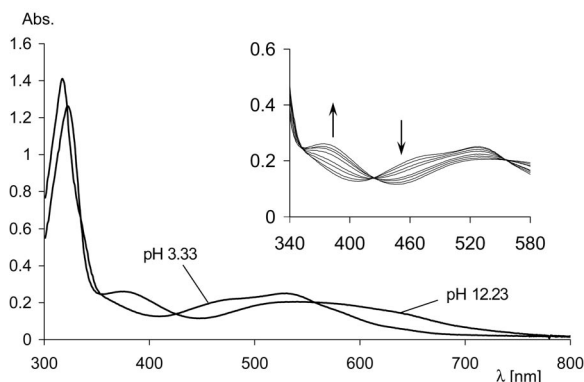


Figure 3. UV/Vis spectra of the aquo and hydroxo forms of complex (S_cS_c, R_aS_a)-**3b** at pH 3.33 and 12.23, respectively. The inset shows a detail of three of the five isosbestic points found from acid-base titration of the aquo complex with NaOH (pH values are 3.3, 8.81, 9.41, 9.60, 10.21, 10.48, 10.88, and 12.23).

The five isosbestic points at $\lambda = 322, 335, 352, 424,$ and 556 nm suggest that the aquo and hydroxo species interconvert in a net way, without generation of any side product. Addition of *p*-toluenesulfonic acid at the end of the titration regenerates the initial aquo complex. The pK_a of 10.45 calculated for the deprotonation of the aquo ligand from acid-base titration is in good agreement with the value extracted from its Pourbaix diagram (see below). The complex (R_cR_c, S_aR_a)-**3a** behaves in an analogous manner, and the UV/Vis spectra of its aquo and hydroxido forms are presented as Supporting Information.

Electrochemical and Catalytic Properties

The redox behavior of the complexes **2a,b-5a,b** and **6b** was studied by cyclic voltammetry. The chlorido complexes (R_cR_c, S_aR_a)-**2a** and (S_cS_c, R_aS_a)-**2b** show a simple chemically and electrochemically reversible wave in acetonitrile, which corresponds to the $\text{Ru}^{\text{III}}/\text{Ru}^{\text{II}}$ couple, at $E_{1/2}$ values of 0.70 and 0.71 V respectively. The analogous pyridine complexes (R_cR_c, S_aR_a)-**5a** and (S_cS_c, R_aS_a)-**5b** undergo an equivalent redox process at higher potential values ($E_{1/2} = 1.15$ and 1.18 V, respectively), which is consistent with the

lower electron-donating capability of the py ligand with regard to the chlorido ligand. Pyridine ligands could, in principle, produce a π -accepting effect involving the empty antibonding orbitals of the aromatic system, although this appears to be negligible for this family of complexes as inferred, as described above, from the NMR and UV/Vis spectra. The π -acceptor nature of the monodentate acetonitrile ligand is significantly manifested in (S_cS_c, R_aS_a)-**4b**, however, which presents a redox potential of 1.22 V.

The 2-OH-py complex (S_cS_c, R_aS_a)-**6b** presents a surprisingly low $E_{1/2}$ value of 0.755 V in dichloromethane. Considering the relatively long Ru–N_{2-OH-py} bond length inferred from DFT calculations^[17] (around 2.23 Å) one would expect a redox potential somewhat higher than those found for pyridine complexes **5a,b** due to the decreased σ donation. The OH group in the ring must therefore play a determinant role in the redox behavior of the complex by stabilizing the Ru^{III} oxidation state through extra σ donation, probably involving deprotonation of the ligand (the pK_a value for 2-OH-py is 0.75) and effective coordination of the corresponding anionic, 2-pyridonyl tautomeric form.

The cyclic voltammograms of the aqua complexes (R_cR_c, S_aR_a)-**3a** and (S_cS_c, R_aS_a)-**3b** were recorded in both dichloromethane and aqueous phosphate buffer solution. Only one redox process, corresponding to the $\text{Ru}^{\text{IV}}/\text{Ru}^{\text{III}}$ redox couple, appears in CH_2Cl_2 at $E_{1/2} = 0.98$ V for both compounds. The intensity decrease or even the disappearance of the $\text{Ru}^{\text{III}}/\text{Ru}^{\text{II}}$ wave for this type of complex in dichloromethane is assigned to kinetic factors and has been described previously for similar complexes.^[21] Two reversible waves, corresponding to the $\text{Ru}^{\text{IV}}/\text{Ru}^{\text{III}}$ and $\text{Ru}^{\text{III}}/\text{Ru}^{\text{II}}$ redox couples, can be observed in aqueous solution (pH 6) at $E_{1/2} = 0.64$ and 0.46 V, respectively, for complex (R_cR_c, S_aR_a)-**3a** and at $E_{1/2} = 0.65$ and 0.46 V, respectively, for (S_cS_c, R_aS_a)-**3b** (the cyclic voltammogram recorded for the latter is provided as Supporting Information).

The difference in the potential values of these two oxidation processes in a specific Ru-aquo complex seems to be directly related to the σ -donor and π -acceptor capacity of the ancillary ligands, as has been described by Meyer and co-workers^[22a] on the basis of some empirical parameters previously calculated by Lever.^[22b] As shown by the authors, two pseudo-linear relationships correlate the difference between the $E_{1/2}$ value for the two oxidation processes, $\Delta E_{1/2}$ (IV/III – III/II), with an empirical coefficient obtained from the ligands coordinated to the metal center (Figure 4). Two groups of compounds can be clearly distinguished depending on the σ -donor or π -acceptor properties of the ligands, denoted with squares and diamonds, respectively, in Figure 4.

The relatively weak π -acceptor character of the oxazoline ligand (with an empirical Lever contribution of 0.21; see the Supporting Information for a detailed description of the calculations) in complexes (R_cR_c, S_aR_a)-**3a** and (S_cS_c, R_aS_a)-**3b** places these complexes in the middle right half of the graph, far away from the central zone for two-electron processes (the aquo complexes described here are represented by a dot in Figure 4).

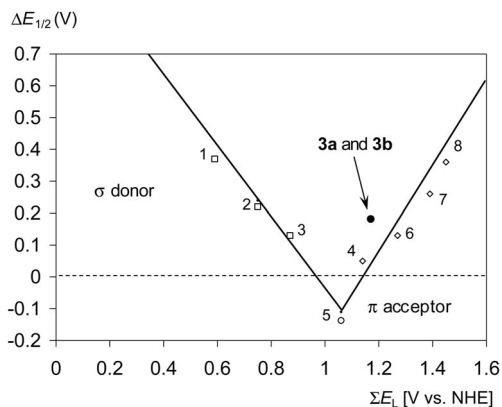


Figure 4. Meyer–Lever plot of $\Delta E_{1/2}$ vs. ΣE_L . [where $\Delta E_{1/2}$ is the difference between the $E_{1/2}(\text{IV/III})$ and $E_{1/2}(\text{III/II})$ redox potentials for the family of complexes studied]. (1) $[\text{Ru}(\text{terpy})(\text{acac})(\text{OH}_2)]^+$; (2) $\text{cis-}[\text{Ru}(\text{terpy})(\text{pic})(\text{OH}_2)]^+$ (pic = picolinate); (3) $[\text{Ru}(\text{terpy})(\text{tmen})(\text{OH}_2)]^{2+}$ (tmen = *N,N,N,N*-tetramethylethylenediamine); (4) $[\text{Ru}(\text{CNC})(\text{bpy})(\text{OH}_2)]^{2+}$ (see ref.^[27]); (5) $[\text{Ru}(\text{CNC})(n\text{BuCN})(\text{OH}_2)]^{2+}$,^[27] (6) $[\text{Ru}(\text{terpy})(\text{bpy})(\text{OH}_2)]^{2+}$ (bpy = 2,2'-bipyridine); (7) $[\text{Ru}(\text{bpy})_2(\text{OH}_2)(\text{PPh}_3)]^{2+}$; (8) $[\text{Ru}(\text{terpy})(\text{dppene})(\text{OH}_2)]^{2+}$ [dppene = *cis*-1,2-bis(diphenylphosphanyl)ethylene].

Generation of the higher oxidation state species was followed spectrophotometrically for the aquo complexes **3a,b**. Figure 5 shows the spectra obtained upon progressive addition of small amounts of Ce^{IV} to an aqueous solution of complex (S_cS_c,R_aS_a) -**3b** at pH 1 until addition of one equivalent. The five isosbestic points observed at $\lambda = 270$, 283, 297, 333, and 420 nm again suggest a net generation of the Ru^{III} species.

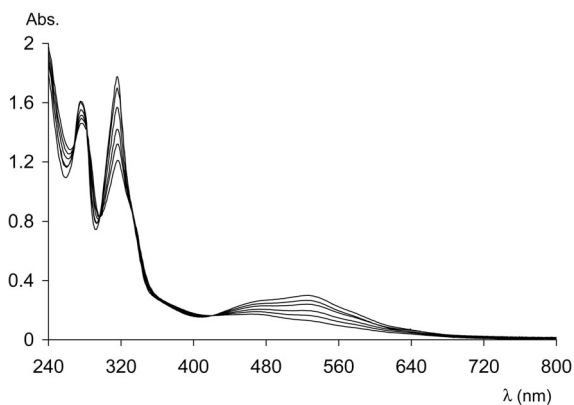
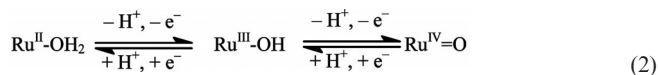


Figure 5. UV/Vis spectra registered after addition of successive amounts of Ce^{IV} (up to 1 equiv.) to a 0.14 mM solution of complex (S_cS_c,R_aS_a) -**3b** in 0.1 M HClO_4 .

Addition of a second equivalent of Ce^{IV} produces a further oxidation of the complex that generates the corresponding Ru^{IV} -oxo species, which is almost featureless in the visible region, as has been described for analogous complexes.^[20d,23] This second redox process also takes place with the presence of isosbestic points, and the manifold of spectra recorded is presented as Supporting Information together with the redox titration of complex (R_cR_c,S_aR_a) -**3a**, which follows a similar trend.

Ruthenium aquo complexes show a pH-dependence of their redox potentials due to deprotonation of the aqua ligand bonded to the metal center [Equation (2)].



This dependence is usually reflected in so-called Pourbaix diagrams, and the results obtained for complex (S_cS_c,R_aS_a) -**3b** are displayed in Figure 6.

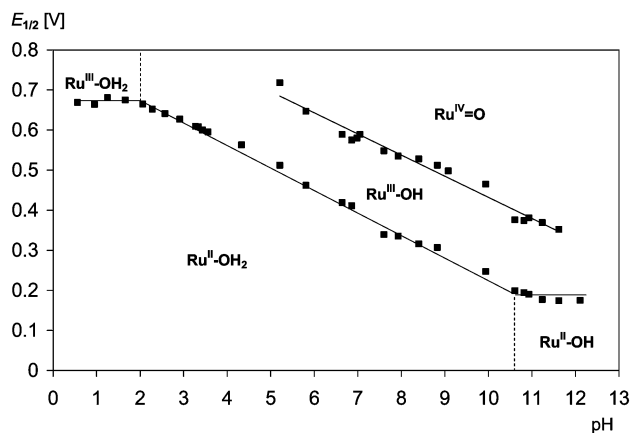


Figure 6. A plot of $E_{1/2}$ vs. pH (Pourbaix diagram) for complex (S_cS_c,R_aS_a) -**3b**. The pH/potential regions of stability for the various oxidation states and their dominant proton compositions are indicated by using abbreviations such as $\text{Ru}^{\text{II}}\text{-OH}_2$, for example, for $[\text{Ru}^{\text{II}}(\text{terpy})(\text{phbox-}i\text{Pr})(\text{H}_2\text{O})]^{2+}$. The pK_a values are shown by the vertical dashed lines in the various $E/p\text{H}$ regions.

The two independent one-electron redox processes that take place with simultaneous proton transfer at pH values between 5 and 10.5 are assignable to $\text{Ru}^{\text{II}} \rightarrow \text{Ru}^{\text{III}}$ and $\text{Ru}^{\text{III}} \rightarrow \text{Ru}^{\text{IV}}$ oxidations. The corresponding lines present a slope of approximately 59 mV per pH unit, as expected for a one-electron one-proton transfer; see Equation (2). At lower pH, only the $\text{Ru}^{\text{III/II}}$ couple can be observed. The diminishment or disappearance of the $\text{Ru}^{\text{IV/III}}$ redox couple in CV experiments is quite common for aquo complexes and is assumed to be caused by slow heterogeneous electron-transfer kinetics from the solution to the electrode surface.^[23a,24] The stability regions for species having different proton composition are indicated in the diagram along with the pK_a values for Ru^{III} and Ru^{II} aquo complexes, which are around 1.93 and 10.44, respectively. The latter value is fully consistent with the value determined from acid-base spectrophotometric titration, as described above.

Complex (R_cR_c,S_aR_a) -**3a** behaves in a similar way to (S_cS_c,R_aS_a) -**3b** (the corresponding Pourbaix diagram is supplied as Supporting Information). In this case, the $\text{Ru}^{\text{IV/III}}$ redox couple can be observed even at a pH lower than 4 and the pK_a values for the $\text{Ru}^{\text{III}}\text{-OH}_2$ and $\text{Ru}^{\text{II}}\text{-OH}_2$ species are 2.1 and 11.1, respectively.

The redox catalytic properties of (S_cS_c,R_aS_a) -**3b** were tested in the electrochemical oxidation of target substrates such as benzyl alcohol and methyl *p*-tolyl sulfide in aqueous

Table 3. Alkene epoxidation catalyzed by (S_cS_c,R_aS_a)-**3b**.^[a]

Entry	Substrate	Oxidant	Substr./cat.	% Conversion	% Epoxide yield	% Bz ^[b] yield	Catalytic cycles
1	styrene	PhI(OAc) ₂	200:1	67.3	36.1	6.1	71.3
2	<i>trans</i> -stilbene	PhI(OAc) ₂	150:1	71	37.4	4.1	57.9
3	styrene	PhIO	200:1	48.9	22.4	10.1	44.1
4	<i>trans</i> -stilbene	PhIO	200:1	74.3	44	29.6	87.6

[a] Reactions were performed at room temperature in 1,2-dichloroethane with an oxidant/substrate molar ratio of 2:1. [b] Bz stands for benzaldehyde.

neutral media. The system “0.5 mM **3b**/50 mM substrate/pH 7 phosphate buffer” at an E_{app} of 0.9 V generated the respective oxidation products (benzaldehyde and sulfoxide) with good selectivities but poor yields (50% and 13% respectively), representing up to 50 and 13 catalytic cycles, after seven hours. No *ee* was observed for the sulfoxide obtained from the prochiral sulfide substrate. The electrocatalytic activity for the oxidation of benzyl alcohol is also visible in the cyclic voltammogram, with an increase in the anodic intensity at lower potential in the presence of the catalyst (see Figure S7 in the Supporting Information). The electrocatalytic oxidation of benzyl alcohol was also tested in a basic medium (0.1 M NaOH; applied potential: 0.5 V); conversions and selectivities were similar to those obtained in a neutral medium.

The catalytic activity of (S_cS_c,R_aS_a)-**3b** was also tested with regard to its ability to epoxidize alkenes. Styrene and *trans*-stilbene were chosen as substrates with PhIO and PhI(OAc)₂ as oxidants in 1,2-dichloroethane; the results, which were quantified by GC chromatography, are reported in Table 3. A first glance shows that the main products formed are the corresponding epoxides (styrene oxide and *trans*-stilbene oxide), along with minor amounts of benzaldehyde, in all cases. However, although good selectivity was achieved for the desired products, the enantioselectivity values for these reactions were low (never higher than 10% *ee*). The selectivity for the epoxide is slightly higher when Ph(IOAc)₂ is used as co-oxidant instead of PhIO (compare for instance entries 2 and 4 in Table 3). *trans*-Stilbene also provides better conversion and epoxide yields than styrene, probably due to the tendency of the latter to undergo double-bond cleavage and polymerization under oxidative conditions.

A potential explanation for this low enantioselectivity can be inferred from the complex structure. The approach of a prochiral substrate to the active site of the catalysts takes place in the region of the planar terpy ligand, therefore the stereogenic center in the oxazoline ligand only has a very small effect on the orientation of the substrate (see Figure 2 and the Supporting Information for different structural views of the molecular catalyst). Thus, the catalyst/substrate interaction can occur through multiple orientations, thereby leading to racemic mixtures of reaction products.

Conclusion

A new family of ruthenium complexes bearing terpy, oxazoline, and a monodentate ligand has been synthesized

and thoroughly characterized. The catalytic activity of the aquo complexes in epoxidation catalysis has been tested. These complexes show moderate activity and chemoselectivity for the epoxide but with only low enantiomeric excesses. We are now working towards the optimization of the reaction conditions by using clean oxidants such as H₂O₂, and also towards a redesign of the catalysts' structures in order to achieve higher enantioselectivities.

Experimental Section

Materials: All reagents used in the present work were obtained from Aldrich Chemical Co and were used without further purification. Reagent-grade organic solvents were obtained from SDS and high purity deionized water was obtained by passing distilled water through a nano-pure Mili-Q water purification system. RuCl₃·2H₂O, was supplied by Johnson–Matthey Ltd. and was used as received.

Instrumentation and Measurements: UV/Vis spectra were recorded with a Cary 50 Scan (Varian) UV/Vis spectrophotometer in 1-cm quartz cells. pH measurements were recorded with a Micro-pH-2000 from Crison.

Cyclic voltammetry (CV) experiments were performed in a PAR 263A EG&G potentiostat or an IJ-Cambria IH-660 potentiostat, using a three-electrode cell. Glassy carbon disk electrodes (3 mm diameter) from BAS were used as the working electrode, platinum wire as the auxiliary electrode, and SSCE as the reference electrode. Cyclic voltammograms were recorded at a scan rate of 100 mV s⁻¹ under either N₂ or Ar. The complexes were dissolved in previously degassed solvents containing the necessary amount of supporting electrolyte to yield a 0.1 M ionic strength solution. (*n*Bu₄N)(PF₆) was used as supporting electrolyte when using acetonitrile and dichloromethane as solvents. In aqueous solutions the pH was adjusted from 0 to 2 with HCl. Sodium chloride was added to keep a minimum ionic strength of 0.1 M. From pH 2 to pH 10, 0.1 M phosphate buffers were used, and from pH 10 to pH 12 dilute, CO₂-free NaOH was used. All $E_{1/2}$ values reported in this work were estimated from cyclic voltammetry as the average of the oxidative and reductive peak potentials ($E_{p,a} + E_{p,c}$)/2. Unless explicitly mentioned, the concentration of the complexes was approximately 1 mM.

Catalytic Experiments: Chemical catalysis was performed using a catalyst:substrate molar ratio of between 1:150 to 1:200, with an oxidant:substrate ration of 2:1, in 1,2-dichloroethane, with a typical catalyst concentration of 1 mM. Electrocatalytic studies at neutral pH were performed in a phosphate buffer solution, at an applied potential of 0.9 V vs. SSCE. At basic pH, a 0.1 M NaOH solution was used as solvent and the potential applied was 0.5 V vs. SSCE. The substrate:catalyst molar ratio was 100:1 in both cases. A carbon-felt electrode from SOFACEL was used as the working electrode. Evolution of the oxidized products was followed with a Shi-

madzu GC-17A gas chromatography apparatus after chromatography of an aliquot of the reaction mixture over alumina and further re-dissolution in a 20 mm biphenyl solution in diethyl ether, which was used as an internal standard.

X-ray Structure Determination: Suitable crystals of (R_cR_c,S_aR_a) -**2b** were grown by slow diffusion of diethyl ether into a dichloromethane solution of the complex at room temperature. They were obtained as black plates. The crystal was mounted on a nylon loop and intensity data were collected at low temperature [100(2) K] with a Bruker Smart Apex CCD diffractometer using graphite-monochromated Mo- K_α radiation ($\lambda = 0.71073 \text{ \AA}$) in the θ range 2.12–28.44°. Full-sphere data collection was carried out with ω and ϕ scans. A total of 48274 reflections were collected, of which 7801 ($R_{\text{int}} = 0.1281$) were unique. Programs used: data collection: Smart version 5.625 (Bruker AXS 1997-01); data reduction: Saint+ version 6.36A (Bruker AXS 2001); absorption correction: SADABS version 2.05 (Bruker AXS 2001). The structures were solved by direct methods and refined by full-matrix least-squares methods on F^2 with SHELXTL Version 6.12 (Bruker AXS 2001). The non-hydrogen atoms were refined anisotropically. All H-atoms were placed in geometrically optimized positions and forced to ride on the atom to which they are attached.

Crystallographic Data for 2b: $C_{33}H_{35}BClF_4N_5O_2Ru$, $M = 756.99$, orthorhombic, space group $P2_12_12_1$, $a = 10.541(2)$, $b = 12.907(3)$, $c = 23.230(5) \text{ \AA}$, $\alpha = 90.00^\circ$, $\beta = 90.00^\circ$, $\gamma = 90.00^\circ$, $V = 3169.5(11) \text{ \AA}^3$, $Z = 4$, $\rho_{\text{calcd.}} = 1.591 \text{ g cm}^{-3}$, $\mu = 0.645 \text{ mm}^{-1}$. Final $R_1 = 0.0822$, $wR_2 = 0.1597$ [$I > 2\sigma(I)$]. $R_1 = \sum ||F_o| - |F_c|| / \sum |F_o|$ and $wR_2 = [\sum \{w(F_o^2 - F_c^2)^2\} / \sum \{w(F_o^2)^2\}]^{1/2}$, where $w = 1/[\sigma^2(F_o^2) + (0.0551P)^2 + 12.3436P]$ and $P = (F_o^2 + 2F_c^2)/3$.

CCDC-635355 contains the supplementary crystallographic data for this paper. These data can be obtained free of charge from The Cambridge Crystallographic Data Center via www.ccdc.cam.ac.uk/data_request/cif.

Preparations: The phbox-R [$R = \text{Et}$, (R_cR_c) -**a**; $i\text{Pr}$, (S_cS_c) -**b**; see Figure 1] ligands^[25] and $[\text{Ru}^{\text{III}}\text{Cl}_3(\text{terpy})]$ (**1**)^[26] (terpy = 2,2':6',2''-terpyridine) were prepared according to literature procedures. The syntheses and specific spectroscopic and electrochemical data for the ruthenium complexes described in this paper {with general formula $[\text{Ru}(\text{Y})(\text{terpy})(\text{phbox-R})]^{n+}$, $\text{Y} = \text{monodentate ligand}$, see below} have been reported previously^[17] but are detailed and discussed here.

The nomenclature used for the absolute configuration of the complexes described is as follows. The first two letters refer to the absolute configuration of the oxazoline ligand and the final two letters refer to the absolute configuration of the chiral rotational axes, as detailed and exemplified in Figure 1 for the chlorido complex **2b**. Thus, the complexes discussed here are (R_cR_c,S_aR_a) - $[\text{RuCl}(\text{terpy})(\text{phbox-et})](\text{BF}_4)$ [(R_cR_c,S_aR_a) -**2a**], (S_cS_c,R_aS_a) - $[\text{RuCl}(\text{terpy})(\text{phbox-}i\text{Pr})](\text{BF}_4)$ [(S_cS_c,R_aS_a) -**2b**], (R_cR_c,S_aR_a) - $[\text{Ru}(\text{terpy})(\text{phbox-et})(\text{OH}_2)](\text{BF}_4)_2$ [(R_cR_c,S_aR_a) -**3a**], (S_cS_c,R_aS_a) - $[\text{Ru}(\text{terpy})(\text{phbox-}i\text{Pr})(\text{OH}_2)](\text{BF}_4)_2$ [(S_cS_c,R_aS_a) -**3b**], (S_cS_c,R_aS_a) - $[\text{Ru}(\text{terpy})(\text{phbox-}i\text{Pr})(\text{MeCN})](\text{PF}_6)_2$ [(S_cS_c,R_aS_a) -**4b**], (S_cS_c,R_aS_a) - $[\text{Ru}(\text{terpy})(\text{phbox-et})(\text{py})](\text{PF}_6)_2$ [(R_cR_c,S_aR_a) -**5a**], (S_cS_c,R_aS_a) - $[\text{Ru}(\text{terpy})(\text{phbox-}i\text{Pr})(\text{py})](\text{PF}_6)_2$ [(S_cS_c,R_aS_a) -**5b**], and (S_cS_c,R_aS_a) - $[\text{Ru}(\text{terpy})(\text{phbox-}i\text{Pr})(2\text{-OH-py})](\text{PF}_6)_2$ [(S_cS_c,R_aS_a) -**6b**].

Supporting Information (see also the footnote on the first page of this article): Additional spectroscopic and electrochemical data for the complexes described in this work.

Acknowledgments

This research was financed by the Spanish Ministerio de Educaci3n y Ciencia (MEC) (projects BQU2003-02884, BQU2002-04112-C02-02, and CTQ2004-01546/BQU). A. L. and M. G. are grateful to the Consell Interdepartamental de Recerca i Innovaci3n Tecnol3gica (CIRIT), Generalitat de Catalunya, for financial support, and A. L. for the aid SGR2001-UG-291. A. L., M. R., and I. R. also thank Johnson Matthey for a loan of $\text{RuCl}_3 \cdot x\text{H}_2\text{O}$. E. P. and X. S. are grateful for the award of doctoral grants from CIRIT and Universitat de Girona (UdG), respectively.

- a) G. Desimoni, G. Faita, K. A. J3rgensen, *Chem. Rev.* **2006**, *106*, 3561–3651; b) A. Landa, A. Minkkila, G. Blay, K. A. J3rgensen, *Chem. Eur. J.* **2006**, *12*, 3472–3483; c) S. Dagorne, S. Bellemin-Lapponnaz, A. Maisse-Fran3ois, *Eur. J. Inorg. Chem.* **2007**, 913–925; d) H. A. McManus, P. J. Guiry, *Chem. Rev.* **2004**, *104*, 4151–4202; e) D. Rechavi, M. Lemaire, *Chem. Rev.* **2002**, *102*, 3467–3493.
- a) H. Brunner, U. Obermann, P. Wimmer, *J. Organomet. Chem.* **1986**, *316*, C1–C3; b) D. A. Evans, K. A. Woerpel, M. M. Hinman, M. M. Faul, *J. Am. Chem. Soc.* **1991**, *113*, 726–728; c) E. J. Corey, N. Imai, H.-Y. Zhang, *J. Am. Chem. Soc.* **1991**, *113*, 728–729.
- a) A. K. Ghosh, M. Packiarajan, J. Cappiello, *Tetrahedron: Asymmetry* **1998**, *9*, 1–45; b) C. Bolm, *Angew. Chem. Int. Ed. Engl.* **1991**, *30*, 542–543.
- M. G3mez, G. Muller, M. Rocamora, *Coord. Chem. Rev.* **1999**, *193–195*, 769–835.
- A. Von Zelewsky, *Stereochemistry of Coordination Compounds*, Wiley, Chichester, **1996**.
- a) F. Leroux, *ChemBioChem* **2004**, *5*, 644–649; b) W. C. Haase, M. Nieger, K. H. Dotz, *J. Organomet. Chem.* **2003**, *684*, 153–169; c) P. Lloyd-Williams, E. Giralt, *Chem. Soc. Rev.* **2001**, *30*, 145–157; d) M. Oki, *Top. Stereochem.* **1983**, *14*, 1–81.
- a) L. Pu, *Chem. Rev.* **1998**, *98*, 2405–2494; b) K. Mikami, K. Aikawa, Y. Yusa, J. J. Jodry, M. Yamanaka, *Synlett* **2002**, 1561–1578.
- a) R. Noyori, *Angew. Chem. Int. Ed.* **2002**, *41*, 2008–2022; b) I. Serrano, M. Rodr3guez, I. Romero, A. Llobet, T. Parella, J. M. Campelo, D. Luna, J. M. Marinas, J. Benet-Buchholz, *Inorg. Chem.* **2006**, *45*, 2644–2651.
- a) D. S. Heseck, Y. Inoue, S. R. L. Everitt, H. Ishida, M. Kuniieda, M. D. Drew, *Inorg. Chem.* **2000**, *39*, 317–324; b) D. Heseck, G. A. Hembury, M. D. Drew, S. Taniguchi, Y. Inoue, *J. Am. Chem. Soc.* **2000**, *122*, 10236–10237; c) R. A. Sheldon, *Chirotechnology*, Marcel Dekker, New York, **1993**; d) P. J. Collins, M. Hird, *Introduction to Liquid Crystals Chemistry and Physics*, Taylor & Francis, London, **1997**.
- See, for instance, cyclopropanation reactions in ref.^[2b] and: a) N. Ostergaard, J. F. Jensen, D. Tanner, *Tetrahedron* **2001**, *57*, 6083–6088; b) T. G. Gant, M. C. Noe, E. J. Corey, *Tetrahedron Lett.* **1995**, *36*, 8745–8748. For allylic substitutions, see: c) M. A. Peric3s, C. Puigjaner, A. Riera, A. Vidal-Ferran, M. G3mez, F. Jim3nez, G. Muller, M. Rocamora, *Chem. Eur. J.* **2002**, *8*, 4164–4178; d) O. Onomura, Y. Kanda, Y. Nakamura, T. Maki, Y. Matsumura, *Tetrahedron Lett.* **2002**, *43*, 3229–3231. For Diels–Alder reactions, see ref.^[2c] and: e) D. A. Evans, T. Rovis, J. S. Johnson, *Pure Appl. Chem.* **1999**, *71*, 1407–1415; f) D. A. Evans, J. A. Murry, P. von Matt, R. D. Norcross, S. J. Miller, *Angew. Chem. Int. Ed. Engl.* **1995**, *34*, 798–800.
- For recent contributions, see: a) D. Carmona, M. P. Lamata, F. Viguri, J. Ferrer, N. Garcia, F. J. Lahoz, M. L. Martin, L. A. Oro, *Eur. J. Inorg. Chem.* **2006**, 3155–3166; b) A. J. Davenport, D. L. Davies, J. Fawcett, D. R. Russell, *J. Organomet. Chem.* **2006**, *691*, 3445–3450; c) M. G3mez, S. Jansat, G. Muller, G. Aullon, M. A. Maestro, *Eur. J. Inorg. Chem.* **2005**, 4341–4351; d) F. Nud, C. Malan, F. Spindler, C. Rugeberg, A. T. Schmidt, H. U. Blaser, *Adv. Synth. Catal.* **2006**, *348*, 47–50; e) H. B. Am-

- mar, J. Le Notre, M. Salem, M. T. Kaddachi, P. H. Dixneuf, *J. Organomet. Chem.* **2002**, *662*, 63–69.
- [12] a) W. Mägerlein, C. Dreisbach, H. Hugl, M. K. Tse, M. Klawonn, S. Bhor, M. Beller, *Catal. Today* **2007**, *121*, 140–150; b) M. K. Tse, H. Jiao, G. Anilkumar, B. Bitterlich, F. G. Gelalcha, M. Beller, *J. Organomet. Chem.* **2006**, *691*, 4419–4433; c) M. K. Tser, S. Bhor, M. Klawonn, G. Anilkumar, H. Jiao, C. Döbler, A. Spannenberg, W. Mägerlein, H. Hugl, M. Beller, *Chem. Eur. J.* **2006**, *12*, 1855–1874; d) M. K. Tser, S. Bhor, M. Klawonn, G. Anilkumar, H. Jiao, C. Döbler, A. Spannenberg, W. Mägerlein, H. Hugl, M. Beller, *Chem. Eur. J.* **2006**, 1875–1888; e) M. K. Tse, C. Döbler, S. Bhor, M. Klawonn, W. Mägerlein, H. Hugl, M. Beller, *Angew. Chem. Int. Ed.* **2004**, *43*, 5255–5260.
- [13] a) R. Ballardini, V. Balzani, A. Credi, M. T. Gandolfi, M. Venturi, *Int. J. Photoenergy* **2001**, *3*, 63; b) E. Baranoff, J.-P. Collin, J. Furusho, Y. Furusho, A. C. Laemmel, J. P. Sauvage, *Inorg. Chem.* **2002**, *41*, 1215–1222.
- [14] a) S. I. Murahashi, H. Takaya, T. Naota, *Pure Appl. Chem.* **2002**, *74*, 19–24; b) T. Naota, H. Takaya, S. I. Murahashi, *Chem. Rev.* **1998**, *98*, 2599–2660; c) U. J. Jauregui-Haza, M. Dessoudeix, P. Kalck, A. M. Wilhelm, H. Delmas, *Catal. Today* **2001**, *66*, 297–302.
- [15] a) S. O. Kelley, J. K. Barton, *Science* **1999**, *238*, 375–381; b) D. B. Hall, R. E. Holmlin, J. K. Barton, *Nature* **1996**, *384*, 731–735; c) C. J. Burrows, J. G. Muller, *Chem. Rev.* **1998**, *98*, 1109–1151.
- [16] a) L. K. Stultz, M. H. V. Huynh, R. A. Binstead, M. Curry, T. J. Meyer, *J. Am. Chem. Soc.* **2000**, *122*, 5984–5996; b) E. L. Lebeau, T. J. Meyer, *Inorg. Chem.* **1999**, *38*, 2174–2181; c) C. M. Che, T. F. Lai, K. Y. Wong, *Inorg. Chem.* **1987**, *26*, 2289–2299; d) J. H. Muller, J. H. Acquaye, K. J. Takeuchi, *Inorg. Chem.* **1992**, *31*, 4552–4557; e) A. Gerli, J. Reedijk, M. T. Lakin, A. L. Spek, *Inorg. Chem.* **1995**, *34*, 1836–1843; f) X. Hua, M. Shang, A. G. Lappin, *Inorg. Chem.* **1997**, *36*, 3735–3740; g) M. Rodríguez, I. Romero, A. Llobet, A. Deronzier, M. Biner, T. Parella, H. Stoeckli-Evans, *Inorg. Chem.* **2001**, *40*, 4150–4156; h) M. Shiotsuki, H. Miyai, Y. Ura, T. Suzuki, T. Kondo, T. Mitsudo, *Organometallics* **2002**, *21*, 4960–4964; i) M. H. V. Huynh, L. M. Witham, J. M. Lasker, M. Wetzler, B. Mort, D. L. Jameson, P. S. White, K. J. Takeuchi, *J. Am. Chem. Soc.* **2003**, *125*, 308–309.
- [17] X. Sala, E. Plantalech, I. Romero, M. Rodríguez, A. Llobet, A. Poater, M. Duran, M. Solà, S. Jansat, M. Gómez, T. Parella, H. Stoeckli-Evans, J. Benet-Buchholz, *Chem. Eur. J.* **2006**, *12*, 2798–2807.
- [18] a) M. Haga, E. S. Dodsworth, A. B. P. Lever, *Inorg. Chem.* **1986**, *25*, 447–453; b) S. C. Rasmussen, S. E. Ronco, D. A. Mlsna, M. A. Billadeau, W. T. Pennington, J. W. Kolis, J. D. Petersen, *Inorg. Chem.* **1995**, *34*, 821–829; c) O. Kohle, S. Ruile, M. Gratzel, *Inorg. Chem.* **1996**, *35*, 4779–4787; d) A. Ben Altabel, S. B. Ribotta de Gallo, M. E. Folquer, N. E. Katz, *Inorg. Chim. Acta* **1991**, *188*, 67–70; e) P. A. Anderson, G. B. Deacon, K. H. Haarmann, F. R. Keene, T. J. Meyer, D. A. Reitsma, B. W. Skelton, G. F. Strouse, N. C. Thomas, T. A. Treadway, A. H. White, *Inorg. Chem.* **1995**, *34*, 6145–6157; f) K. Barqawi, A. Llobet, T. J. Meyer, *J. Am. Chem. Soc.* **1988**, *110*, 7751–7759.
- [19] L. F. Szczepura, S. M. Maricich, R. F. See, M. R. Churchill, K. J. Takeuchi, *Inorg. Chem.* **1995**, *34*, 4198–4205.
- [20] a) N. Chanda, S. M. Mobin, V. G. Puranik, A. Datta, M. Niemeyer, G. K. Lahiri, *Inorg. Chem.* **2004**, *43*, 1056–1064; b) C. Sens, M. Rodríguez, I. Romero, A. Llobet, T. Parella, J. Benet-Buchholz, *Inorg. Chem.* **2003**, *42*, 8385–8394; c) B. Mondal, V. G. Puranik, G. K. Lahiri, *Inorg. Chem.* **2002**, *41*, 5831–5836; d) K. J. Takeuchi, M. S. Thompson, D. W. Pipes, T. J. Meyer, *Inorg. Chem.* **1984**, *23*, 1845–1851; e) L. Roecker, W. Kutner, J. A. Gilbert, M. Simmons, R. W. Murray, T. J. Meyer, *Inorg. Chem.* **1985**, *24*, 3784–3791.
- [21] a) W. F. De Giovani, A. Deronzier, *J. Electroanal. Chem.* **1992**, *337*, 285–298; b) M. Rodríguez, I. Romero, C. Sens, A. Llobet, A. Deronzier, *Electrochim. Acta* **2003**, *48*, 1047–1054.
- [22] a) A. Dovletoglou, S. A. Adeyemi, T. J. Meyer, *Inorg. Chem.* **1996**, *35*, 4120–4127; b) A. B. P. Lever, *Inorg. Chem.* **1990**, *29*, 1271–1285.
- [23] a) J. C. Dobson, T. J. Meyer, *Inorg. Chem.* **1988**, *27*, 3283–3291; b) A. Llobet, P. Doppelt, T. J. Meyer, *Inorg. Chem.* **1988**, *27*, 514–520; c) W. C. Cheng, W. Y. Yu, K. K. Cheung, C. M. Che, *J. Chem. Soc. Dalton Trans.* **1994**, 57–62; d) M. E. Marmion, K. J. Takeuchi, *J. Am. Chem. Soc.* **1986**, *108*, 510–511; e) S. A. Kubow, M. E. Marmion, K. J. Takeuchi, *Inorg. Chem.* **1988**, *27*, 2761–2767.
- [24] a) G. E. Cabaniss, A. A. Diamantis, W. R. Murphy, R. W. Linton, T. J. Meyer, *J. Am. Chem. Soc.* **1985**, *107*, 1845–1853; b) V. J. Catalano, R. Kurtaran, R. A. Heck, A. Ohman, M. G. Hill, *Inorg. Chim. Acta* **1999**, *286*, 181–188.
- [25] C. Bolm, K. Weickhard, M. Zehnder, D. Glasmacher, *Chem. Ber.* **1991**, *124*, 1173–1180.
- [26] B. P. Sullivan, J. M. Calvert, T. J. Meyer, *Inorg. Chem.* **1980**, *19*, 1404–1407.
- [27] E. Masllorens, M. Rodríguez, I. Romero, A. Roglans, T. Parella, J. Benet-Buchholz, M. Poyatos, A. Llobet, *J. Am. Chem. Soc.* **2006**, *128*, 5306–5307.

Received: April 4, 2007

Published Online: September 28, 2007